ELEMENTA
Science of the Anthropocene

Etiope, G and Schwietzke, S. 2019. Global geological methane emissions: An update of top-down and bottom-up estimates. *Elem Sci Anth,* 7: 47. DOI: https://doi.org/10.1525/elementa.383

RESEARCH ARTICLE

Global geological methane emissions: An update of top-down and bottom-up estimates

Giuseppe Etiope* and Stefan Schwietzke†

A wide body of literature suggests that geological gas emissions from Earth's degassing are a major methane (CH_4) source to the atmosphere. These emissions are from gas-oil seeps, mud volcanoes, microseepage and submarine seepage in sedimentary (petroleum-bearing) basins, and geothermal and volcanic manifestations. Global bottom-up emission estimates, ranging from 30 to 76 Tg CH_4 yr^{-1}, evolved in the last twenty years thanks to the increasing number of flux measurements, and improved knowledge of emission factors and area distribution (activity). Based on recent global grid maps and updated evaluations of mud volcano and microseepage emissions, the global geo-CH_4 source is now (bottom-up) estimated to be 45 (27–63) Tg yr^{-1}, i.e., ~8% of total CH_4 sources. Top-down verifications, based on independent approaches (including ethane and isotopic observations) from different authors, are consistent with the range of the bottom-up estimate. However, a recent top-down study, based on radiocarbon analyses in polar ice cores, suggests that geological, fossil (^{14}C-free) CH_4 emissions about 11,600 years ago were much lower (<15 Tg yr^{-1}, 95% CI) and that this source strength could also be valid today. Here, we show that (i) this geo-CH_4 downward revision implies a fossil fuel industry CH_4 upward revision of at least 24–35%. (ii) The 95% CI estimates of the recent radiocarbon analysis do not overlap with those of 5 out of 6 other bottom-up and top-down studies (no overlap for the 90% CI estimates). (iii) The contrasting lines of evidence require further discussion, and research opportunities exist to help explain this gap.

Keywords: Geological methane; Seepage; Global emission estimates; Bottom-up; Top-down

1. Introduction

Methane is an important greenhouse gas, and our understanding of the magnitude and trends of its sources and sinks is incomplete at best (Kirschke et al., 2013; Saunois et al., 2016; Rice et al., 2016; Schaefer et al., 2016; Nisbet et al., 2016; Schwietzke et al., 2016; Worden et al., 2017; Rigby et al., 2017; Turner et al., 2017). Quantifying source and sink attributions, between anthropogenic and natural sources, but also within anthropogenic sources, is key for designing mitigation strategies and estimating their climate impacts (Nisbet et al., 2019). Earth's degassing is considered a major natural source of methane (CH_4) to the atmosphere, as discussed in a wide body of literature (e.g., Lacroix, 1993; Etiope and Klusman, 2002; Judd et al., 2002; Kvenvolden and Rogers, 2005; Etiope et al., 2019). CH_4 degassing occurs through five main categories of surface gas manifestations: gas-oil seeps, mud volcanoes, microseepage, submarine seepage, and geothermal and volcanic manifestations. These are defined and described in detail, for example, in Judd et al. (2002), Dimitrov (2003), Etiope and Klusman, (2010), Mazzini and Etiope (2017), Etiope (2015) and Etiope et al. (2019), and references therein.

The global CH_4 emissions from these sources have been mainly estimated through bottom-up procedures by various authors (see **Table 1**), based on process-based modelling, statistical evaluations of experimentally determined emission factors and activity data (number of emission points or emission area) and inventories. Global geo-CH_4 emission estimates (including all five geo-CH_4 categories) range from 30 to 76 Tg yr^{-1}, with a typical mean around 50 Tg yr^{-1} (**Table 1**). As shown in detail below, top-down emission estimates, based on present-day atmospheric data of isotopic (^{14}C and $^{13}C/^{12}C$) CH_4 composition or ethane (C_2H_6) emissions (also derived from polar ice cores), are consistent with the order of magnitude of the bottom-up estimates (Etiope et al., 2008; Schwietzke et al., 2016; Nicewonger et al., 2016; Dalsøren et al., 2018). Differently, Petrenko et al. (2017) proposed a substantially lower global estimate, ranging from 0 (zero) to 15.4 Tg yr^{-1} (95% CI). This range was derived from radiocarbon (^{14}C) measurements in CH_4 trapped in ice cores in Antarctica and referring to the atmosphere of 11,000–12,000 years ago, between the Younger Dryas and Preboreal intervals. Assuming that geological emissions today are not higher (or even lower) than in the analysed period, Petrenko et al. (2017) concluded that previous present-day geo-CH_4 estimates of ~50 Tg yr^{-1} are overestimated. As stated in Petrenko et al. (2017), this geo-CH_4 downward revision also implies an upward

* Istituto Nazionale di Geofisica e Vulcanologia, Rome, IT
† Environmental Defense Fund, London, UK
Corresponding author: Giuseppe Etiope (giuseppe.etiope@ingv.it)

revision of the present-day fossil fuel industry CH_4 emission estimates.

The objectives of this paper are: (1) Combine and reasses the most recent global bottom-up geo-CH_4 emission estimates based on recently published global grid maps and updated inventories discussed in Etiope et al. (2019). (2) Summarize top-down emission estimates by combining data from Schwietzke et al. (2016), Nicewonger et al. (2016), Saunois et al. (2016) and Dalsøren et al. (2018), followed by a calculation of the average ethane/methane (C_2/C_1) ratio for the five geological sources (having specific C_2/C_1 ratios, as reported in Etiope and Ciccioli, 2009). Based on this overview of geo-CH_4 top-down emission estimates using multiple species, datasets, and methods, the discrepancy between these estimates and the range proposed by Petrenko et al. (2017) is addressed. (3) Discuss and quantify in more detail the fossil fuel industry CH_4 upward revision proposed by Petrenko et al. (2017). (4) Offer suggestions for further research activities to reconcile the above discrepancies, and to better constrain geological emission estimates.

2. Bottom-up geo-CH_4 emission estimates

The objective of the recently published globally gridded dataset of geo-CH_4 emissions (Etiope et al., 2019) was to develop the first comprehensive a priori emission grid for atmospheric modelling. The gridding work allowed refining the CH_4 emission estimates for mud volcanoes and microseepage, thanks to a better assessment of their activity (global area) and emission factors (Etiope et al., 2019). These new estimates are reported in **Table 2**. However, these grid maps do not represent the entire global geo-CH_4 source because for some categories of geo-CH_4 sources, namely onshore gas-oil seeps, submarine seepage and geothermal emissions, the datasets used for the spatial gridding (developed for modelling purposes) are incomplete or do not contain the information necessary for improving all previous estimates.

The following provides a brief summary of the gridded geo-CH_4 estimates (Etiope et al., 2019) as well as the other previous global geo-CH_4 total estimates from the literature (**Table 1**). Note that the approaches used to quantify emission uncertainties vary among the different bottom-up studies given the different spatial scales (global total vs. grid-level uncertainties) as described below. In most cases, however, best estimates of lower and upper bounds were reported, and these ranges are summarized here.

2.1. Updates based on gridded geo-CH_4 estimates

The CH_4 emission range of mud volcanoes, 3.9–8.3 (mean 6.1) Tg yr^{-1}, combines uncertainties of the mud volcano areas and emission factors (Etiope et al., 2019). The mud volcano areas were estimated using image (Google Earth) analysis, photos and published literature (uncertainty of 6%) and the emission factors were based on regression analysis between area and seepage flux for 16 mud volcanoes measured in Europe and Asia (uncertainty of about 42%; Etiope et al., 2019).

The emission range of microseepage, 15–33 (mean 24) Tg yr^{-1}, reflects an uncertainty of about 38% estimated through analysis of sensitivity of the microseepage model (based on geospatial and statistical analyses) used to derive the global microseepage emission (Etiope et al., 2019). Briefly, the microseepage emission factors are based on a statistical analysis of a dataset of 1509 flux measurements (acquired by accumulation chamber method) from 19

Table 1: Global bottom-up geo-CH_4 emission estimates (Tg yr^{-1}) from literature. DOI: https://doi.org/10.1525/elementa.383.t1

Reference	Tg yr^{-1}	
Etiope and Klusman (2002)	30–70	
Judd et al. (2002)	13–36	*microseepage not included*
Kvenvolden and Rogers (2005)	45	
Etiope et al. (2008)	42–64	
Etiope (2015)	45–76	
Etiope et al. (2019)	43–50	*extrapolation from grid maps*

Table 2: Improved global bottom-up emission estimates for the five geo-CH_4 sources (Tg yr^{-1}) by combining literature estimates (Table 1) and recent updates from Etiope et al. (2019). DOI: https://doi.org/10.1525/elementa.383.t2

	mean	min	max	Reference
Onshore mud volcanoes	6.1	3.9	8.3	Etiope et al. (2019)
Onshore gas-oil seep	3.5	3	4	Etiope et al. (2008a)
Submarine seepage	7	3	10	Judd (2004); Etiope et al. (2019)
Microseepage	24	15	33	Etiope et al. (2019)
Geothermal-volcanic manifestations	4.7	2.2	7.3	Etiope (2015)
Total	**~45**	**~27**	**~63**	

different petroliferous basins, associated with geological factors (macro-seeps, faults, seismicity) that can influence the microseepage intensity (Etiope et al., 2019); the microseepage area (activity) was estimated using the global area of petroleum fields and macro-seeps (which may occur also outside a petroleum field) and knowing, from the global microseepage dataset, that microseepage (positive CH_4 fluxes) occurs in about 57% of the petroleum field area (Etiope et al., 2019). The sensitivity of the model was tested by combining different emission factors (median, geometric mean, upper and lower 95% confidence limit) and activity (microseepage area 20% smaller or higher).

Concerning the global submarine emissions, which only refers to waters shallower than 500 m where emitted methane can reach the atmosphere, a new range is suggested combining data from Etiope et al. (2019) and previous estimates (Kvenvolden et al. 2001; Judd, 2004). Etiope et al. (2019) report a partial dataset (15 areas) of local and regional emission estimates, totally resulting in 1.8–6.0 (mean 3.9) Tg yr^{-1}. They estimate that other 16 areas may release an additional ~1 Tg yr^{-1}. In these areas, gas was observed to reach the sea surface via bubble plumes, but the output to the atmosphere was not provided. This yields a global submarine emission range of ~3–7 Tg yr^{-1}. Previous estimates are those reported by Kvenvolden et al. (2001), where a range of 10–30 Tg yr^{-1} was proposed (see also Judd, 2004). The partial emission dataset reported in Etiope et al. (2019) includes major submarine seepage areas investigated so far, but may be a conservative (low) estimate. Nevertheless, it suggests that global submarine emissions may not exceed the minimum value of 10 Tg yr^{-1} by Kvenvolden et al. (2001). Therefore, until further data emerge, the range 3–10 Tg yr^{-1} is proposed here as a best guess.

2.2. Literature estimates for other geo-CH_4 categories

Gridding work in Etiope et al. (2019) did not result in new estimates from onshore gas-oil seeps and geothermal manifestations. The most detailed global total emission estimates from these two geo-CH_4 categories are still those from previous statistical and process-based modeling (Etiope et al., 2008a; Etiope, 2015; **Table 2**).

Global CH_4 emission estimates from gas-oil seeps, 3–4 (mean 3.5) Tg yr^{-1}, were based on a database of fluxes that were measured directly (typically by accumulation chamber method) from 66 gas seeps in 12 countries, assuming that their flux and size distributions were representative of the global gas-oil seep population (Etiope et al., 2008a). The global emission range reflects an uncertainty of about 15% estimated combining two different extrapolations of emission factors over the global number of seeps (Etiope et al., 2008a). Global CH_4 emission estimates from geothermal manifestations, 2.2–7.3 (mean 4.7) Tg yr^{-1}, were derived on the basis of the most updated estimates of global CO_2 emissions from volcanic areas (540 Tg yr^{-1}), from non-volcanic areas (300–1,000 Tg yr^{-1}), and a wide dataset on CO_2/CH_4 compositional ratios in both areas (Etiope 2015 and references therein). The emission range reflects an uncertainty of about 53% derived from the uncertainty of non-volcanic CO_2 emissions (Etiope 2015; the uncertainty of volcanic CO_2 degassing was not quantified in the original work; Burton et al., 2013).

In summary, considering the updates based on gridded geo-CH_4 estimates and literature estimates for the other geo-CH_4 categories, the global bottom-up geological CH_4 emission is now estimated at ~45 (27–63) Tg yr^{-1} (**Table 2**). Note that this estimate uses the best individual estimates presently available for the five geo-CH_4 source categories, while the global estimate proposed in Etiope et al. (2019) refers to the global emissions "extrapolated" from gridded maps (**Table 1**). As explained above, the extrapolation from gridded maps contains incomplete information on oil-gas seeps, submarine and geothermal emissions. Although derived through different approaches the two estimates are however similar.

3. Top-down geo-CH_4 emission estimates

Top-down geo-CH_4 emission estimates can be derived via multiple approaches, based on the present-day fraction of radiocarbon (^{14}C) free CH_4 in the atmosphere (Lassey et al., 2007), pre-industrial ethane (C_2H_6) and CH_4 isotopic composition in polar ice cores and box modelling (Nicewonger et al., 2016; Schwietzke et al., 2016; Dalsøren et al., 2018). Similar to the bottom-up approaches described above, the way the reporting of emission uncertainties varies among studies given the different methodologies (e.g., atmospheric forward modelling of set emission scenarios vs. inverse or box modelling with explicit posterior uncertainties). When only lower and upper bounds were reported, then these ranges are summarized here.

3.1. Present day ^{14}C approach

Lassey et al. (2007) deduced that 30% ± 2.3% (1 SD) of the global CH_4 source for 1986–2000 is ^{14}C-free (and thus fossil), although they considered this "a plausible re-estimate rather than a definitive revision" of previous lower fossil CH_4 estimates (on average 20%). Taking into account the average top-down total CH_4 source of 560 Tg yr^{-1} (reported by Saunois et al., 2016 and valid for the period 1986–2000, as indicated by Lassey et al., 2007) yields 168 Tg yr^{-1} total fossil CH_4 emissions, i.e., natural (geological) plus anthropogenic (fossil fuel industry sources including CH_4 venting and leaks). Using the range of the fossil fuel industry fraction reported in the average bottom-up and top-down estimates by Saunois et al. (2016), i.e., 101–134 Tg yr^{-1}, yields geological emission range of 34–67 (mean 50.5) Tg yr^{-1}.

3.2. Pre-industrial $^{13}C/^{12}C$ approach

The box modelling by Schwietzke et al. (2016), based on CH_4 concentration and isotopic data from ice-core records suggest geo-CH_4 emissions of 31–71 Tg yr^{-1} (1 SD, mean 51 Tg yr^{-1}). These estimates consider a new database of present-day $^{13}C/^{12}C$ signatures for all CH_4 sources, and assume that these signatures are also representative of the pre-industrial era. The relatively wide geo-CH_4 range is partly due to a wide range of prescribed biomass burning CH_4 emissions from present-day estimates. The central value, 51 Tg yr^{-1}, is consistent with the above estimate combining Lassey et al. (2007) and Saunois et al. (2016) data. Note

that this wide geo-CH_4 uncertainty range is largely due to uncertainties in pre-industrial biomass burning CH_4 baseline emission estimates (i.e., long-term averages), but it is unrelated to current-day uncertainties the trend of burning CH_4 emissions (Worden et al., 2017).

3.3. Present day $^{13}C/^{12}C$ and inventory approach

With the same box model plus 3-D forward modelling, but using present-day atmospheric CH_4 and isotopic data, Schwietzke et al. (2016) suggested a total fossil (geological plus fossil fuel industry) CH_4 source of 150–200 Tg yr^{-1}. Considering the fossil fuel industry emission estimates of Saunois et al. (2016) above, i.e., 101–134 Tg yr^{-1}, requires geo-CH_4 emissions of 16–99 Tg yr^{-1} (minimum-maximum range). Note that the global total CH_4 source budget in Saunois et al. (2016) is ~5% less than in Schwietzke et al. (2016) due to slightly different assumptions in the CH_4 sink magnitude. As a result, the above geo-CH_4 emission estimate of 16–99 Tg yr^{-1} may be a slight underestimate.

3.4. Pre-industrial C_2H_6 approach

Based on pre-industrial concentrations of C_2H_6 in polar ice cores, Nicewonger et al. (2016) estimated total geological C_2H_6 emissions of 2.2–3.5 Tg yr^{-1}, which is consistent with previous estimates of 2–4 Tg yr^{-1} proposed by Etiope and Ciccioli (2009). Additional ethane ice core data and modelling suggests that geo-C_2H_6 emissions could be even higher (5–6 Tg yr^{-1}; Nicewonger et al., 2018). Considering here the conservative range of Nicewonger et al. (2016), we estimate the total geo-CH_4 emission estimate using global averages of ethane/methane (C_2/C_1) ratios from geological sources (reported in Etiope and Ciccioli, 2009). An average, emission-weighted geological C_2/C_1 ratio can be derived taking into account the emission fraction of the five geological sources identified in **Table 2**. A C_2H_6 source of 2.2–3.5 Tg yr^{-1} (Nicewonger et al., 2016) requires a CH_4 source in the range of 29–46 (mean 37.5) Tg yr^{-1} (**Table 3**).

3.5. Present day C_2H_6 approach

Based on C_2H_6 observations and simulations with a detailed atmospheric-chemistry transport model, Dalsøren et al. (2018) estimated total geological C_2H_6 emissions of 2–4 Tg yr^{-1}, similar to Nicewonger et al. (2016) and Etiope and Ciccioli (2009). In this case, using the same C_2/C_1 ratio estimated above, yields global CH_4 emissions in the range of 27–52 (mean 39.5) Tg yr^{-1} (**Table 3**).

3.6. Summary of all approaches above

All geo-CH_4 emission estimates are then summarized in **Figure 1**, which categorizes studies into Petrenko et al. (2017), bottom-up, top-down C_2H_6-based, and the other top-down studies discussed above. For Petrenko et al. (2017), the 95% confidence interval and range of mean values in **Figure 1** are as reported in that study. For bottom-up, we used the minimum and maximum values from **Table 2** as described in Section 2. We then assumed a uniform distribution around the minimum and maximum values to calculate 95% confidence intervals and the standard deviation. Note that assuming a uniform distribution is conservative in the sense that the 95% confidence intervals extend closer to the underlying minimum and maximum values compared to, e.g., Gaussian or triangular distributions. In other words, the lack of overlap in 95% confidence intervals between Petrenko et al. (2017) and the bottom-up approach would be even more pronounced if instead a Gaussian or triangular distribution was assumed.

Top-down C_2H_6-based 95% confidence intervals were calculated from the joint probability distribution of Nicewonger et al. (2016) and Dalsøren et al. (2018) by performing a Monte Carlo simulation (N = 10,000) giving equal weight to each study, and also assuming a uniform

Table 3: Derivation of global geo-CH_4 emission (Tg yr^{-1}) from geo-ethane emission estimates. DOI: https://doi.org/10.1525/elementa.383.t3

	C_2/C_1 ratio[a]	C_1 emission[b] (Tg yr^{-1})	Em. fraction
Mud volcanoes	0.0007	6.1	0.13
Gas-oil seeps	0.0182	3.5	0.08
Submarine seepage	0.0120	7	0.15
Microseepage	0.0684	24	0.53
Geothermal manifestations	0.0130	4.7	0.10
Total		45.3	
Emission-weighted mean	0.0429		
	C_2 emission (Tg yr^{-1})	**C_1 emission (Tg yr^{-1})**	
min Nicewonger et al. (2016)	2.2	29	
max Nicewonger et al. (2016)	3.5	46	
min Dalsøren et al. (2018)	2	27	
max Dalsøren et al. (2018)	4	52	

[a] C_2/C_1 ratios from Etiope and Ciccioli (2009).
[b] Emissions from Table 1.

distribution using each study's minimum and maximum values. The colored dots show the 95% confidence intervals of Nicewonger et al. (2016) and Dalsøren et al. (2018) individually. The same approach was used for the top-down "other" category representing Lassey et al. (2007), Saunois et al. (2016), and Schwietzke et al. (2016) as described above. Note that the 95% confidence intervals of Petrenko et al. (2017) only overlap with those of Schwietzke et al. (2016), not with those of the other studies or the three categories. The overlap in the 95% confidence intervals represents the intersection of the extreme ends of both distributions (90% confidence intervals do not overlap; the range is 18–83 Tg yr^{-1} in Schwietzke et al., 2016). Further, the right side of the 95% confidence interval in Petrenko et al. (2017) is a factor of 3 to 6 lower than all other studies.

For illustration, averaging the mean values of the bottom-up and top-down estimates and using their full range of 95% confidence interval uncertainties in **Figure 1** (excluding those in Petrenko et al., 2017) results in a global geo-CH_4 emission range of ~28–75 (mean 45) Tg yr^{-1}. In **Figure 2**, this value is compared with other natural and anthropogenic CH_4 sources. Only combining the lowest

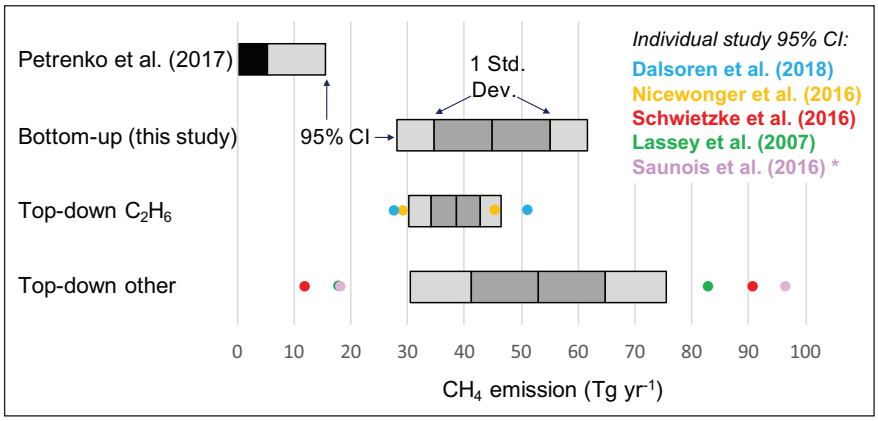

Figure 1: Comparison of geo-CH_4 emission estimates (Tg yr^{-1}) based on different data and quantification approaches. The black bar (Petrenko et al., 2017) indicates the range of mean values (including zero) from the five different periods analyzed (Younger Dryas-Preboreal transition), and the light gray bar indicates the 95% confidence interval. The remaining bars represent summary statistics from the bottom-up approach as well as from the joint probability distributions (see text) of the ethane-based top-down studies and the other top-down studies. Specifically, light gray bars represent 95% confidence intervals, and dark gray bars represent 1 standard deviation (including mean values in the center). The colored dots indicate the 95% confidence intervals of each individual study within each top-down category. * See text for estimating geo-CH_4 emissions based on Saunois et al. (2016) data. DOI: https://doi.org/10.1525/elementa.383.f1

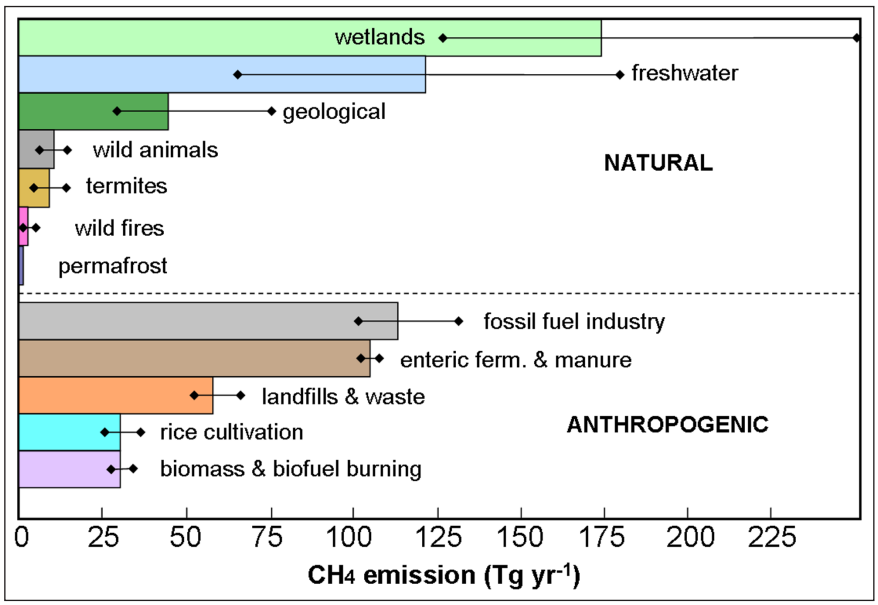

Figure 2: Comparison between current day estimates of geological and other methane sources. Geological emissions are based on the bottom-up and top-down estimates discussed in this work (see Fig. 1 and text). Other natural and anthropogenic emissions refer to the average (and range) of bottom-up and top-down estimates reported by Saunois et al. (2016). Note that a downward revision of the geological source requires an upward revision of the same magnitude for the fossil fuel industry (Section 4). DOI: https://doi.org/10.1525/elementa.383.f2

estimates from different authors, the global geo-CH_4 emission would be 18 Tg yr^{-1} (see **Table 6** in Etiope et al., 2019) and compatible with the upper limit of Petrenko et al. (2017).

4. Implications of a geo-CH_4 downward revision on fossil fuel industry CH_4 estimates

Present-day total fossil CH_4 emissions have been estimated top-down using $^{13}C/^{12}C$ and ^{14}C data as described above, but these approaches alone do not attribute emissions between the geo-CH_4 source and the fossil fuel industry CH_4 source. Separate geo-CH_4 estimates (bottom-up and top-down, Sections 2 and 3) have been used to then infer the fossil fuel industry CH_4 source. As noted in Petrenko et al. (2017), a geo-CH_4 downward revision thus necessitates a fossil fuel industry CH_4 upward revision to satisfy the present-day $^{13}C/^{12}C$ and ^{14}C constraints.

Consider a geo-CH_4 source of 46 Tg yr^{-1} (mean of bottom-up and top-down estimates, Section 3), and a total fossil fuel CH_4 source of 172 Tg yr^{-1} (mean of $^{13}C/^{12}C$ and ^{14}C estimates, Section 3). This implies a fossil fuel industry CH_4 source of 126 Tg yr^{-1} (consistent with the upper end of recently revised bottom-up estimates of Saunois et al., 2016; Section 3). A geo-CH_4 downward revision to 0–15 Tg yr^{-1} (estimate by Petrenko et al., 2017) thus requires a fossil fuel industry CH_4 upward revision to 157–172 Tg yr^{-1}, which is 24–35% larger than previous estimates. Note that the percentage range would increase if lower fossil fuel industry CH_4 emission estimates were used as a baseline, e.g., the lower bottom-up range in Saunois et al. (2016).

5. Temporal variation of geological methane sources

While all bottom-up and top-down estimates, following independent techniques from different authors, have similar ranges, suggesting a global geo-CH_4 emission source in the order of 40–50 Tg yr^{-1}, the radiocarbon (^{14}C-CH_4) data in ice cores reported by Petrenko et al. (2017) revise these estimates downward, with a range of 0 (zero) to 18.1 Tg yr^{-1} (<15.4 Tg yr^{-1}, 95% CI) at least for the atmosphere between 11,000 and 12,000 years ago (Younger-Dryas Preboreal transition). Petrenko et al. (2017) assumed that those past geological emissions are not lower than today, claiming therefore that the previous present-day geo-CH_4 estimates are too high.

The assumption that geological emissions are constant over the Holocene is not necessarily correct. Earth's degassing, which is a process mainly driven by gas advection, is basically controlled by gas pressure gradients in the subsurface and permeability of fractured rocks. These factors can vary considerably on short time scales, in relation, for example, to cycles of gas pressure discharges and build-up in reservoirs, seismic activity, mud volcano eruptions, hydraulic pressure of aquifers and neotectonic stresses (e.g., Quigley et al., 1999; Yang et al., 2006; Delisle et al., 2010; Etiope, 2015). Episodes of enhanced mud volcanism, for example, were recognised in the Upper Quaternary (Etiope et al., 2008b). Modern formation of new mud volcanoes and seeps is documented in several countries (Etiope, 2015). Combinations of such temporal variations at regional scale may lead to a significant variation of the global emission.

Similarly, it is not clear whether during the Younger-Dryas Preboreal transition a wider cover of ice and permafrost may have "capped" and lowered a significant portion of seepage in the boreal hemisphere (as a potential explanation for the discrepancy in geo-CH_4 estimates).

6. How geological CH_4 emission estimates can be better constrained

We identify two major lines of research that can better constrain the geo-CH_4 emission estimates: (a) CH_4 flux derivation of large active seeps and mud volcanoes based on atmospheric in-situ measurements or remote sensing; (b) improving the definition of global microseepage area.

(a) The existence of mud volcanoes, which alone are estimated to emit ~6 Tg yr^{-1} (**Table 2**), provides a unique opportunity for direct measurements that could test the hypothesis of near-zero global geo-CH_4 emissions. Twenty–five of the world's largest mud volcanoes are located in a relatively small region surrounding the Caspian Sea, and they emit an estimated 1.5 Tg yr^{-1} in aggregate (Etiope et al., 2019). The individual mud volcanoes can be considered point sources with spatial dimensions comparable to oil and gas production and processing facilities. Their emission estimates can thus be empirically verified using "fence-line" downwind measurement methodologies employed during oil and gas methane field measurements over the last decade in the US and internationally (Alvarez et al., 2018). Similarly, the advancement of space-based remote sensing instruments could lead to the flux quantification of the entire region described above. This, however, also requires source attribution of geo-CH_4 and other CH_4 sources. The 1.5 Tg yr^{-1} represents only a relatively small fraction of the bottom-up estimated global geo-CH_4 source. However, verifying emission estimates from these mud volcanoes represents a check on the overall bottom-up method that is applied similarly for other seepage categories, and simultaneously a check on the near-zero emission hypothesis of the radiocarbon-based geo-CH_4 downward revision.

(b) Based on statistical treatment of emission factor and activity (area) data, microseepage is considered the largest geo-CH_4 source (10–25 Tg yr^{-1}; Etiope and Klusman, 2010; 24 ± 9 Tg yr^{-1}; Etiope et al., 2019). Its main uncertainty is due to the limited knowledge of the actual global area where microseepage occurs. Ground-based measurements (soil-gas and flux data) and remote sensing surveys (multispectral imagery) demonstrated that every petroleum field investigated so far is characterized by areas of microseepage, especially at the boundary of the field (Klusman et al., 1998; Etiope and Klusman, 2010; Asadzadeh and de Souza Filho, 2017 and references therein). Flux measurements (1509 data from 19 petroleum fields) showed that microseepage occurs in at least half of the petroleum field area (Etiope et al., 2019). A review of remote sensing investigations, preferably with new data, could allow to better

assess the statistics of microseepage in petroleum fields and then globally, as the global area of petroleum fields is known (Etiope et al., 2019).

Data Accessibility Statement

No new measurements were made for this article. All datasets discussed and elaborated in the text are from published scientific literature.

Acknowledgements

We thank the three anonymous reviewers whose comments helped to substantially improve the paper.

Funding information

The work was supported by NASA grant NNX17AK20G.

Competing interests

The authors have no competing interests to declare.

Author contributions

- Contributed to conception and design: GE and SS
- Contributed to analysis and interpretation of data: GE and SS
- Drafted and/or revised the article: GE and SS
- Approved the submitted version for publication: GE and SS

References

Alvarez, RA, Zavala-Araiza, D, Lyon, DR, Allen, DT, Barkley, ZR, Brandt, AR, Davis, KJ, Herndon, SC, Jacob, DJ, Karion, A, Kort, EA, Lamb, BK, Lauvaux, T, Maasakkers, JD, Marchese, AJ, Omara, M, Pacala, SW, Peischl, J, Robinson, AL, Shepson, PB, Sweeney, C, Townsend-Small, A, Wofsy, SC and **Hamburg, SP.** 2018. Assessment of methane emissions from the U.S. oil and gas supply chain. *Science* **361**: 186–188. DOI: https://doi.org/10.1126/science.aar7204

Asadzadeh, S and **de Souza Filho, CR.** 2017. Spectral remote sensing for onshore seepage characterization: A critical overview. *Earth-Science Reviews* **168**: 48–72. DOI: https://doi.org/10.1016/j.earscirev.2017.03.004

Burton, MR, Sawyer, GM and **Granieri, D.** 2013. Deep carbon emissions from volcanoes. *Rev Mineral Geochem* **75**: 323–354. DOI: https://doi.org/10.2138/rmg.2013.75.11

Dalsøren, SB, Myhre, G, Hodnebrog, Ø, Myhre, CL, Stohl, A, Pisso, I, Schwietzke, S, Höglund-Isaksson, L, Helmig, D, Reimann, S, Sauvage, S, Schmidbauer, N, Read, KA, Carpenter, JJ, Lewis, AC, Punjabi, S and **Wallasch, M.** 2018. Discrepancy between simulated and observed ethane and propane levels explained by underestimated fossil emissions. *Nature Geosci* **11**: 178–184. DOI: https://doi.org/10.1038/s41561-018-0073-0

Delisle, G, Teschner, M, Faber, E, Panahi, B, Guliev, I and **Aliev, C.** 2010. First approach in quantifying fluctuating gas emissions of methane and radon from mud volcanoes in Azerbaijan. In: Wood, L (ed.), Shale Tectonics. *Amer. Assoc. Petrol. Geol. Memoir* **93**: 209–222.

Dimitrov, L. 2003. Mud volcanoes – a significant source of atmospheric methane. *Geo-Mar Lett* **23**: 155–161. DOI: https://doi.org/10.1007/s00367-003-0140-3

Etiope, G. 2015. *Natural Gas Seepage. The Earth's hydrocarbon degassing*, 199. Switzerland: Springer. DOI: https://doi.org/10.1007/978-3-319-14601-0

Etiope, G and **Ciccioli, P.** 2009. Earth's degassing – A missing ethane and propane source. *Science* **323**(5913): 478. DOI: https://doi.org/10.1126/science.1165904

Etiope, G, Ciotoli, G, Schwietzke, S and **Schoell, M.** 2019. Gridded maps of geological methane emissions and their isotopic signature. *Earth Syst Sci Data* **11**: 1–22. DOI: https://doi.org/10.5194/essd-11-1-2019

Etiope, G and **Klusman, RW.** 2002. Geologic emissions of methane to the atmosphere. *Chemosphere* **49**: 777–789. DOI: https://doi.org/10.1016/S0045-6535(02)00380-6

Etiope, G and **Klusman, RW.** 2010. Microseepage in drylands: Flux and implications in the global atmospheric source/sink budget of methane. *Global Planet Change* **72**: 265–274. DOI: https://doi.org/10.1016/j.gloplacha.2010.01.002

Etiope, G, Lassey, KR, Klusman, RW and **Boschi, E.** 2008a. Reappraisal of the fossil methane budget and related emission from geologic sources. *Geoph Res Lett* **35**: L09307. DOI: https://doi.org/10.1029/2008GL033623

Etiope, G, Milkov, AV and **Derbyshire, E.** 2008b. Did geologic emissions of methane play any role in Quaternary climate change? *Global Planet Change* **61**: 79–88. DOI: https://doi.org/10.1016/j.gloplacha.2007.08.008

Judd, AG. 2004. Natural seabed seeps as sources of atmospheric methane. *Environ Geol* **46**: 988–996. DOI: https://doi.org/10.1007/s00254-004-1083-3

Judd, AG, Hovland, M, Dimitrov, LI, Garcia, GS and **Jukes, V.** 2002. The geological methane budget at continental margins and its influence on climate change. *Geofluids* **2**: 109–126. DOI: https://doi.org/10.1046/j.1468-8123.2002.00027.x

Kirschke, S, Bousquet, P, Ciais, P, Saunois, M, Canadell, JG, Dlugokencky, EJ, Bergamaschi, P, Bergmann, D, Blake, DR, Bruhwiler, L, Cameron-Smith, P, Castaldi, S, Chevallier, F, Feng, L, Fraser, A, Heimann, M, Hodson, EL, Houweling, S, Josse, B, Fraser, PJ, Krummel, PB, Lamarque, J-F, Langenfelds, RL, Quéré, CL, Naik, V, O'Doherty, S, Palmer, PI, Pison, I, Plummer, D, Poulter, B, Prinn, RG, Rigby, M, Ringeval, B, Santini, M, Schmidt, M, Shindell, DT, Simpson, IJ, Spahni, R, Steele, LP, Strode, SA, Sudo, K, Szopa, S, van der Werf, GR, Voulgarakis, A, van Weele, M, Weiss, RF, Williams, JE and **Zeng, G.** 2013. Three decades of global methane sources 49 and sinks. *Nature Geoscience* **6**: 813–823. DOI: https://doi.org/10.1038/ngeo1955

Klusman, RW, Jakel, ME and **LeRoy, MP.** 1998. Does microseepage of methane and light hydrocarbons contribute to the atmospheric budget of methane and to global climate change? *Assoc. Petrol. Geochem. Explor. Bull.* **11**: 1–55.

Kvenvolden, KA, Lorenson, TD and **Reeburgh, W.** 2001. Attention turns to naturally occurring methane seepage. *EOS* **82**: 457. DOI: https://doi.org/10.1029/01EO00275

Kvenvolden, KA and **Rogers, BW.** 2005. Gaia's breath global methane exhalations. *Mar Petrol Geol* **22**: 579–590. DOI: https://doi.org/10.1016/j.marpetgeo.2004.08.004

Lacroix, AV. 1993. Unaccounted-for sources of fossil and isotopically enriched methane and their contribution to the emissions inventory: A review and synthesis. *Chemosphere* **26**: 507–557. DOI: https://doi.org/10.1016/0045-6535(93)90441-7

Lassey, KR, Lowe, DC and **Smith, AM.** 2007. The atmospheric cycling of radiomethane and the "fossil fraction" of the methane source. *Atmos Chem Phys* **7**: 2141–2149. DOI: https://doi.org/10.5194/acp-7-2141-2007

Mazzini, A and **Etiope, G.** 2017. Mud volcanism: An updated review. *Earth Sci Rev* **168**: 81–112. DOI: https://doi.org/10.1016/j.earscirev.2017.03.001

Nicewonger, MR, Ayding, M, Prather, MJ and **Saltzman, ES.** 2018. Large changes in biomass burning over the last millennium inferred from paleoatmospheric ethane in polar ice cores. *PNAS* **115**: 12413–12418. DOI: https://doi.org/10.1073/pnas.1807172115

Nicewonger, MR, Verhulst, KR, Aydin, M and **Saltzman, ES.** 2016. Preindustrial atmospheric ethane levels inferred from polar ice cores: A constraint on the geologic sources of atmospheric ethane and methane. *Geoph Res Lett* **43**: 1–8. DOI: https://doi.org/10.1002/2015GL066854

Nisbet, EG, Dlugokencky, EJ, Manning, MR, Lowry, D, Fisher, RE, France, JL, Michel, SE, Miller, JB, White, JWC, Vaughn, B, Bousquet, P, Pyle, JA, Warwick, NJ, Cain, M, Brownlow, R, Zazzeri, G, Lanoisellé, M, Manning, AC, Gloor, E, Worthy, DEJ, Brunke, E-G, Labuschagne, C, Wolff, EW and **Ganesan, AL.** 2016. Rising atmospheric methane: 2007–2014 growth and isotopic shift. *Global Biogeochemical Cycles* **30**: 1356–1370. DOI: https://doi.org/10.1002/2016GB005406

Nisbet, EG, Manning, MR, Dlugokencky, EJ, Fisher, RE, Lowry, D, Michel, SE, Myhre, CL, Platt, SM, Allen, G, Bousquet, P, Brownlow, R, Cain, M, France, JL, Hermansen, O, Hossaini, R, Jones, AE, Levin, I, Manning, AC, Myhre, G, Pyle, JA, Vaughn, BH, Warwick, NJ and **White, JWC.** 2019. Very strong atmospheric methane growth in the 4 years 2014–2017: Implications for the Paris Agreement. *Global Biogeochemical Cycles* **33**. DOI: https://doi.org/10.1029/2018GB006009

Petrenko, VV, Smith, AM, Schaefer, H, Riedel, K, Brook, E, Baggenstos, D, Harth, C, Hua, Q, Buizert, C, Schilt, A, Mitchell, L, Bauska, T, Orsi, A, Weiss, RF and **Severinghaus, JP.** 2017. Minimal geological methane emissions during the Younger Dryas–Preboreal abrupt warming event. *Nature* **548**: 443–446. DOI: https://doi.org/10.1038/nature23316

Quigley, DC, Hornafius, JS, Luyendyk, BP, Francis, RD, Clark, J and **Washburn, L.** 1999. Decrease in natural marine hydrocarbon seepage near Coal Oil Point, California, associated with offshore oil production. *Geology* **27**: 1047–1050. DOI: https://doi.org/10.1130/0091-7613(1999)027<1047:DINMHS>2.3.CO;2

Rice, AL, Butenhoff, CL, Teama, DG, Röger, FH, Khalil, MAK and **Rasmussen, RA.** 2016. Atmospheric methane isotopic record 6 favors fossil sources flat in 1980s and 1990s with recent increase. *PNAS* **113**: 10791–10796. DOI: https://doi.org/10.1073/pnas.1522923113

Rigby, M, Montzka, SA, Prinn, RG, White, JWC, Young, D, O'Doherty, S, Lunt, M, Ganesane, AL, Manningf, A, Simmondsa, P, Salamehg, PK, Harthg, CM, Mühleg, J, Weissg, RF, Fraserh, PJ, Steeleh, LP, Krummelh, PB, McCullocha, A and **Parki, S.** 2017. Role of atmospheric oxidation in recent methane growth. *PNAS* **114**: 5373–5377. DOI: https://doi.org/10.1073/pnas.1616426114

Saunois, M, Bousquet, P, Poulter, B, Peregon, A, Ciais, P, Canadell, JG, Dlugokencky, EJ, Etiope, G, Bastviken, D, Houweling, S, Janssens-Maenhout, G, Tubiello, FN, Castaldi, S, Jackson, RB, Alexe, M, Arora, VK, Beerling, DJ, Bergamaschi, P, Blake, DR, Brailsford, G, Brovkin, V, Bruhwiler, L, Crevoisier, C, Crill, P, Curry, C, Frankenberg, C, Gedney, N, Höglund-Isaksson, L, Ishizawa, M, Ito, A, Joos, F, Kim, H-S, Kleinen, T, Krummel, P, Lamarque, J-F, Langenfelds, R, Locatelli, R, Machida, T, Maksyutov, S, McDonald, KC, Marshall, J, Melton, JR, Morino, I, Naik, V, O'Doherty, S, Parmentier, F-JW, Patra, PK, Peng, C, Peng, S, Peters, GP, Pison, I, Prigent, C, Prinn, R, Ramonet, M, Riley, WJ, Saito, M, Santini, M, Schroeder, R, Simpson, IJ, Spahni, R, Steele, P, Takizawa, A, Thornton, BF, Tian, H, Tohjima, Y, Viovy, N, Voulgarakis, A, van Weele, M, van der Werf, G, Weiss, R, Wiedinmyer, C, Wilton, DJ, Wiltshire, A, Worthy, D, Wunch, DB, Xu, X, Yoshida, Y, Zhang, B, Zhang, Z and **Zhu, Q.** 2016. The Global Methane Budget 2000–2012. *Earth Syst Sci Data* **8**: 697–751. DOI: https://doi.org/10.5194/essd-8-697-2016

Schaefer, H, Fletcher, SEM, Veidt, C, Lassey, KR, Brailsford, GW, Bromley, TM, Dlugokencky, EJ, Michel, SE, Miller, JB, Levin, I, Lowe, DC, Martin, RJ, Vaughn, BH and **White, JWC.** 2016. A 21st century shift from fossil-fuel to biogenic methane emissions indicated by 13CH4. *Science* **352**: 80–84. DOI: https://doi.org/10.1126/science.aad2705

Schwietzke, S, Sherwood, OA, Bruhwiler, LMP, Miller, JB, Etiope, G, Dlugokencky, EJ, Michel, SE, Arling, VA, Vaughn, BH, White, JWC and

Tan, PP. 2016. Upward revision of global fossil fuel methane emissions based on isotope database. *Nature* **538**: 88–91. DOI: https://doi.org/10.1038/nature19797

Turner, AJ, Frankenberg, C, Wennberg, PO and **Jacob, DJ.** 2017. Ambiguity in the causes for decadal trends in atmospheric methane and hydroxyl. *PNAS* **114**(21): 5367–5372. DOI: https://doi.org/10.1073/pnas.1616020114

Worden, JR, Bloom, AA, Pandey, S, Jiang, Z, Worden, HM, Walker, TW, Houweling, S and **Röckmann, T.** 2017. Reduced biomass burning emissions reconcile 34 conflicting estimates of the post-2006 atmospheric methane budget. *Nature Communications* **8**: 2227. DOI: https://doi.org/10.1038/s41467-017-02246-0

Yang, TF, Fu, CC, Walia, V, Chen, CH, Chyi, LL, Liu, TK, Song, SR, Lee, M, Lin, CW and **Lin, CC.** 2006. Seismo-geochemical variations in SW Taiwan: Multiparameter automatic gas monitoring results. *Pure Appl. Geophys.* **163**: 693–709. DOI: https://doi.org/10.1007/s00024-006-0040-3

How to cite this article: Etiope, G and Schwietzke, S. 2019. Global geological methane emissions: An update of top-down and bottom-up estimates. *Elem Sci Anth,* 7: 47. DOI: https://doi.org/10.1525/elementa.383

Domain Editor-in-Chief: Detlev Helmig, Institute of Alpine and Arctic Research, University of Colorado Boulder, US

Associate Editor: Paul Palmer, School of GeoSciences, The University of Edinburgh, UK

Knowledge Domain: Atmospheric Science

Part of an *Elementa* Forum: Oil and Natural Gas Development: Air Quality, Climate Science, and Policy

Submitted: 19 May 2019 **Accepted:** 22 October 2019 **Published:** 19 November 2019

ELEMENTA Science of the Anthropocene

Elem Sci Anth is a peer-reviewed open access journal published by University of California Press.

OPEN ACCESS